# Solid-shell element model of assumed through-thickness electric distribution for laminate composite piezoelectric structures

Sung Yi[1,*] and Lin Quan Yao[1]

[1] *School of mechanical and Production Engineering, Nanyang Technological University, Singapore 639798, Republic of Singapore*
[1] *Singapore-MIT Alliance,*
*School of mechanical and Production Engineering, Nanyang Technological University, Singapore 639798*
*And National University of Singapore, E4-04-10, 4 Engineering Drive 3, Singapore 117576, Republic of Singapore*

***Abstract*** — The eight-node solid-shell finite element models have been developed for the analysis of laminated composite pate/shell structures with piezoelectric actuators and sensors. To resolve the locking problems of the solid-shell elements in laminated materials and improve accuracy, the assumed natural strain method and hybrid stress method are employed. The nonlinear electric potential distribution in piezoelectric layer is described by introducing internal electric potential. The developed finite element models, especially, electric potential node model, have the advantages of simpler modeling and can obtain same effect that exact solution described.

***Keywords*** — Laminate composite structure, Piezoelectric material, Finite element method, hybrid stress element.

## 1. INTRODUCTION

The piezoelectric materials have attracted significant attention among the research community for their potential application as sensors for monitoring and as actuators for controlling the response of structures because of their coupled mechanical and electrical properties. For smart structures, experimental models and prototypes are limited to relatively simple structures, such as beams and plates. Thus, in practical applications, finite element techniques provide the versatilities in modeling, simulation, and analysis of engineering designs in modern smart/intelligent material and structures. There have been many theories and models proposed for the analysis of laminated composite plates containing active and passive piezoelectric layers [1-10]. Owing to the geometric complexity of the surface bonded sensors and actuators which are most conveniently be modelled by continuum elements (no rotational d.o.f.), many of the developed finite element models are continuum in nature [8-10]. However, strict considerations of locking deficiencies are often lacking in the course of developing these finite element models. It is unfortunate that solid elements when applied to plate and shell analyses can be plagued by the largest number of finite element deficiencies which include shear, membrane, trapezoidal, thickness and dilatational lockings. Moreover, on piezoelectric element, most of researcher use simplifying approximations attempting to replicate the induced electric field generated by a piezoelectric layer under an external electric field or applied load. Generally, they assume that the electric potential distribution varies linearly in through-thickness of piezoelectric layer. But, According to the results of the exact solution of reference [11] and cantilever bimorph beam which will get in following section, the electric field distribution in piezoelectric layer is not constant.

In this paper, we shall start with an eight-node hybrid stress and assumed strain (ANS) solid-shell element for laminate composite structures. it is applicable to thin plate/shell analyses without suffering the afore-mentioned lockings [5]. The element is then generalized for modeling piezoelectric material. The concept of the electric nodes is introduced that can effectively eliminate the burden of constraining the equality of the electric potential for the nodes lying on the same metallization. In order to model the practical through-thickness electric field distribution in piezoelectric layer, assume the electric potential distribution varies second-order through-thickness

in the piezoelectric layer by introducing internal electric potential of piezoelectric element. Several examples are considered by the new finite element models and compared with exact solution and other predicted results to illustrate their accuracy and efficacy in smart structure modeling.

## 2. ASSUMED NATURAL SHEAR AND THICKNESS STRAINS

Figure 1 shows an eight-node hexahedral element in which ξ, η and ζ are the natural coordinates. Let ζ be aligned with the transverse direction of the shell, the geometric and displacement interpolation [illegible] expressed as:

[illegible] (1)

[illegible] (2)

where, [illegible] ’s are the two-dimensional 4-node Lagranging interpolation functions, **X**, [illegible] and [illegible] are the coordinate vectors, its value at the [illegible] and [illegible] nodes of the element, respectively. **U**, [illegible] and [illegible] are the displacement vector with respect to the global Cartesian coordinates, its value at the [illegible] and [illegible] nodes of the element, respectively.

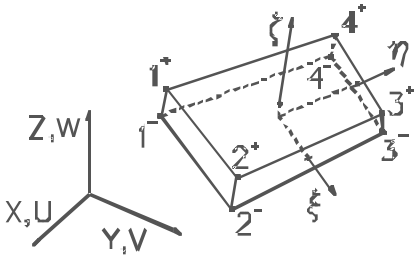


Figure1. An eight-node thin hexahedral solid element.

The strain-displacement relation of the element by incorporating the commonly employed geometric assumptions in shells will be presented. With reference to the interpolations of **X** and **U**, the infinitesimal covariant or natural element strain [illegible] components are:

[illegible]

[illegible]

[illegible]

[illegible] ,

It has rather been a standard practice to use ANS, assumed natural strain, method for resolving the shear locking, trapezoidal locking and the constant moment patch test failure in the present element configuration [5]. The following approximations are adopted accordingly for the three covariant element [illegible] strain components:

[illegible] (4)

As the material properties are often defined in a local orthogonal frame x-y-z, it is necessary to obtain the local physical strains from the covariant ones. It will be assumed as usual that the z-axis and the x-y-plane are parallel to the ζ-axis and mid-surface of the shell, respectively. Hence, the relations between the covariant strains and the local physical strains when approximated by the ones [illegible] evaluated at the mid-surface are [13]

[illegible] (5)

where [illegible] , [illegible] , [illegible] , [illegible] , [illegible] , and are the unit vectors along the local x-, y- and z-directions.

By consolidating equation (3) to equation (5), and the first and second order ζ–terms are truncated in transverse shear strains and the tangential strains respectively, thus the physical [illegible] strains can be expressed symbolically as:

[illegible] , (6)

where [illegible] , [illegible] . **B**’s are independent of ζ and $\mathbf{q}^e$ is the element displacement vector.

## 3. SOLID-SHELL ELEMENT FOR PIEZOELECTRIC PATCHES

In the following, we give the relation between electric field and electric potential. The most of researcher assume that the electric potential distribution varies linearly through-thickness in piezoelectric layer. But, an exact solution for piezoelectric laminate plates has shown that the electric potential distribution is nonlinear [11].We can also show this fact through the following cantilever bimorph beam. This bimorph pointer is portrayed in Figure 2. It consists of two identical PVDF layers with vertical but opposite polarities and, hence, will bend when a load at the end of the beam is applied vertically.

Opened-circuit electric condition (electric displacement equal zero) is used, and let Possion ratio $\nu = 0$ and piezoelectric coefficient for simplification. Thus, the constitutive relations between axial strain , stress and electric field are expressed as

$$\qquad\qquad (7)$$

in which the symbol denote piezoelectric coefficient of upper layer and lower layer, respectively. According the mechanics of material,

$$\qquad\qquad (8)$$

where $P$ is load at the free end of the beam. $L$, $b$ and $h$ are the length, width and thickness of the beam respectively.

From above equations, electric field and electric potential can be obtained as following

$$\qquad , \qquad\qquad (9)$$

here assume connective surface between both layer is zero electric potential. From above equations (9), it is shown that electric field and electric potential are linear and second order function with thickness direction ($z$), respectively, instead of constant and linear distribution that most researcher assumed, as shown as Figure 3 and 4.

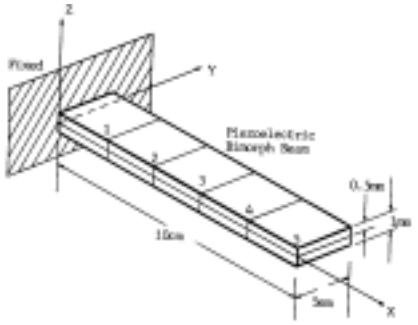


Figure 2. Piezoelectric polymeric bimorph beam

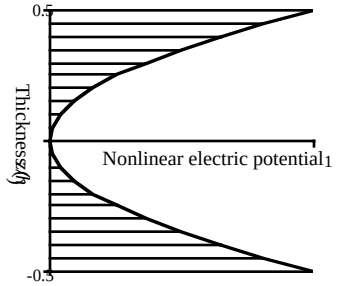


Figure 3. Through-thickness electric potential distribution

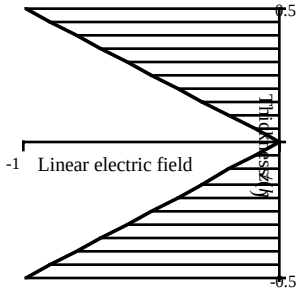


Figure 4. Through-thickness electric field distribution

Moreover, the electric potential distributed in piezoelectric material is generally function of place space. But, practically, electropolar direction is perpendicular to in-plane of the piezoelectric patch as sensor and/or actuator. Thus, the same piezoelectric patch/film (i.e. it has same electrode) has same electric potential on its same surface. For generic piezoelectric solid elements, each node are equipped with three translations and one electric potential as the nodal d.o.f.s. It would be necessary to constraint the equality of the electric d.o.f.s of the nodes on the same electrode. To avoid this tedious task, the electric d.o.f.s are separated from the kinetic nodes with which kinetic d.o.f.s are associated. Then, all elements modelling the same piezoelectric patch/film share the same electric node. Unlike kinetic nodes, electric nodes have no coordinates. Figure 5 shows two elements that model the same piezoelectric patch and they only need three electric d.o.f.s, which are grouped under

distribution in piezoelectric layer, assume the electric potential distribution varies second-order through-thickness in the piezoelectric layer by introducing internal electric potential of piezoelectric element. Then, electric potential can be expressed as:

(10)

where, , , and are, respectively, the top, bottom and internal electric potential of the piezoelectric node. The electric field in the transverse direction with respect to the local Cartesian system is derived from above potential expression as

(11)

where is the electric field-electric potential matrix in the transverse direction.

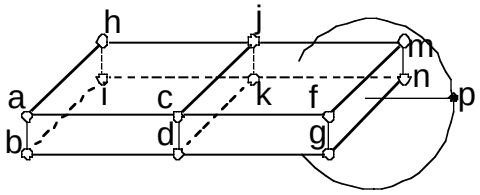


Figure 5. The solid elements modelling the same piezoelectric patch/film share the same electric node, i.e.,connectivity for l.h. element : [ a, c, j, h, b, d, k, i, p ]; connectivity for r.h. element : [ c, f, m, j, d, g, n, k, p]

Without sacrificing much generality for plates/shells, transverse shear response is assumed to be uncoupled from the others. And, with two of the electric field components vanished and the poling direction always aligned with the transverse direction, the piezoelectric constitutive relation can be expressed as :

(12)

where

, contain the piezoelectric coefficients, and are the electric displacement and the permittivity coefficient in the transverse direction, respectively.

## 4. SOLID-SHELL ELEMENT FOR LAMINATED MATERIALS

The thickness average of the thickness strain can be calculated by first re-writing equation (12) as:

(13)

where, , , and are independent of , and the element thickness stress will be assumed to be independent of ζ. For higher computational efficiency, the second order ζ-terms in the inplane strain are often truncated whereas only the zero order ζ-term is retained in the Jacobian determinant that following will turn up. Substituting equations (11) to (13) we have

(14)

where

( , $k$ = 0,1 or 2)

The & , ’s and ’s will be termed as the modified generalized laminate stiffness matrix that relates the generalized element stress and element strain, the generalized piezo-strain coefficients and the generalized permittivity coefficient in the transverse direction, respectively. Note that , the following process is then dealt with . By using of the following generalized elementwise potential energy functional:

(15)

where $P^e$ is the element load potential due to mechanical force and surface charge. in which $J$ is the Jacobian determinant, in general, a quadratic polynomial of ζ. Form above equation (15), following static equations of the piezoelectric elementwise are derived as

(16)

is the elementwise mechanical force due to the body force and surface traction, is the elementwise electric force vector due to the charge density.

## 5. HYBRID STRESS SOLID-SHELL ELEMENT FOR LAMINATED MATERIALS

To apply hybrid stress (HS) formulation to the above ANS solid-shell element as a means to improve the in-plane response, the following elementwise modified Hellinger-Reissner functional can be invoked [14]:

(17)

where , and .

The following orthogonal constant and non-constant stress modes are chosen in a way similar that of Pian’s eight-node element [15-16]:

(18)

Substituting equation (18) into equation (17) and by used of equations (6) and (11), after condensing β’s with the stationary conditions of with respect to β’s, the elementwise static equation can be obtained. It has the same form with equation but the elements of matrix should be

## 6. SYSTEM EQUATION

Assembling the elemental matrices gives the global system matrices. The resulting dynamic becomes

(19)

where **M** is the mass matrix. is the proportional passive damping matrix. **q**, Φ and are the system vectors of nodal displacement, electric potentials, respectively; **F**$_f$ and **F**$_Q$ are the assembled counterparts of and , respectively. The internal DOF can be condensed from the system equations in order to improve the computation efficiency. One can obtain the ed matrix equations as

(20)

.

For an eigenvalue analysis, the undamped eneous system matrices are used, i.e.

(21)

To improve the computational efficiency, the unspecified potentials can be condensed from the system matrices. Thus, a standard eigenvalue can be obtained as

(22)

Eigenvalues and mode shapes can be calculated and defined accordingly.

If the actuators and sensors are partitioned in structure, it is convenient to partition the system vector of electric potential into that of the actuators and of the sensors . In particular, is block diagonal because the host structure is non-piezoelectric, i.e. and do not couple. As there is no electric loading applied to the sensors, vanishes. Consequently, equation (20) split into:

(23)

(24)

(25)

where

[illegible]

[illegible]

[illegible]

Equation (25) gives sensor outputs and can be processed to provide input signals to the actuators for active vibration control. Substitution of equation (25) into equation (23) results in :

[illegible]

(26)

With the control algorithm known and by virtue of equation (24), can be expressed in terms of **q** and thus all the electric d.o.f.s in equation (26) can be condensed.

## 7. NUMERICAL EXAMPLES

The free-vibration responses and electric potential mode of simply supported square plates with surface bonded continuous piezoelectric players are analyzed by using of two finite element methods, namely, displacement method described in section 4, denoted as ANS, and hybrid stress method described in section 5, denoted as HS.

The plates studied are square with simply supported edges. Three different lamination schemes are considered. The first has the layer of [1/2/2/1], and second [2/1/1/2], where digitals 1 and 2 denote the orthotropic PVDF and the transversely isotropic PZT-4, respectively, as shown as Table 1. Each layer has equal thickness of 0.25$h$, where $h$ is the total thickness of the laminated plate. The third has the five-ply laminate [p/0/90/0/p]. The laminate configuration consists of a [0/90/0] Gr/Epoxy, denoted as 4 in Table 1, cross-ply sub-laminate with composite plies each 0.8$h$/3 thick. Two continuous PZT-4, denoted as 2 in Table1, layers of thickness 0.1$h$ each are also bonded to the upper and lower surfaces of the laminate. To comply with the reported results of exact solution, all layers were assumed to have equal density ($\rho$=1kg/m$^3$). Two aspect ratios of thick plate ($a/h$=4) and thin plate ($a/h$=50) are considered, where letter $a$ denotes the length of the square plate. The outer surfaces of the piezoelectric layers were forced to remain always grounded. Based on this, two sets of electric boundary conditions were considered for the inner surface of the piezoelectric layers: a closed-circuit condition (O), where the electric potential remains free (zero electric displacements).

TABLE 1

MATERIAL PROPERTIES ($\varepsilon_0$=8.85 10$^{-12}$ farad/m)

| Property | 1 | 2 | 3 | 4 |
|---|---|---|---|---|
| Elastic: | | | | |
| $E_1$(GPa) | 237.0 | 81.3 | 63.0 | 132.38 |
| $E_2$ | 23.2 | 81.3 | 63.0 | 10.756 |
| $E_3$ | 10.5 | 64.5 | 63.0 | 10.756 |
| $G_{44}$ | 2.15 | 25.6 | 24.231 | 3.606 |
| $G_{55}$ | 4.4 | 25.6 | 24.231 | 5.6537 |
| $G_{66}$ | 6.43 | 30.6 | 24.231 | 5.6537 |
| $v_{12}$ | 0.154 | 0.329 | 0.3 | 0.24 |
| $v_{13}$ | 0.178 | 0.432 | 0.3 | 0.24 |
| $v_{23}$ | 0.177 | 0.432 | 0.3 | 0.49 |
| Piezoelectric | | | | |
| $e_{31}$(C/m$^2$) | -0.13 | -5.20 | 44.367 | 0 |
| $e_{32}$ | -0.14 | -5.20 | 44.367 | 0 |
| $e_{33}$ | -0.28 | 15.08 | 50.182 | 0 |
| $e_{24}$ | -0.01 | 12.72 | 14.151 | 0 |
| Permittivity | | | | |
| $\varepsilon_{11}/\varepsilon_0$ | 12.5 | 1475 | 1728.8 | 0 |
| $\varepsilon_{22}/\varepsilon_0$ | 11.98 | 1475 | 1728.8 | 0 |
| $\varepsilon_{33}/\varepsilon_0$ | 11.98 | 1300 | 6362.7 | 0 |

*Fundamental natural frequency*. The normalized natural frequencies by using of the exact results [11] for the first and third laminated schemes plates are shown in Table 2 to Table 3. FER in Table 3 denotes the finite element results in reference [3] in the case of three discrete-layers. According to the Tables 2 to 3, the predicted natural frequencies by means of both displacement element and hybrid-stress element methods consistently converge above and below the values of the exact solution depending on the type of electric boundary conditions for both thick and thin plates. The differences between both methods in all results are very small.

TABLE 2

THE NORMALIZED NATURAL FREQUENCIES OF THREE LAYERS PIEZOELECTRIC PLATE [1/2/2/1]

| aspect ratios | | $a/h$=4 | | $a/h$=50 | |
|---|---|---|---|---|---|
| mesh | method | (C) | (O) | (C) | (O) |
| | ANS | 1.046 | 1.046 | 1.074 | 1.074 |

| | | | | | |
|---|---|---|---|---|---|
| 8×8 | ANS | 1.006 | 1.006 | 1.014 | 1.014 |
| | HS | 1.005 | 1.005 | 1.014 | 1.014 |
| 12×12 | ANS | 0.998 | 0.998 | 1.004 | 1.004 |
| | HS | 0.998 | 0.998 | 1.003 | 1.003 |

TABLE 3

THE NORMALIZED NATURAL FREQUENCIES OF FIVE-PLY COMPOSITE PIEZOELECTRIC PLATE [p/0/90/0/p]

| aspect ratios | | *a*/*h*=4 | | *a*/*h*=50 | |
|---|---|---|---|---|---|
| mesh | method | (C) | (O) | (C) | (O) |
| 4×4 | ANS | 1.040 | 1.058 | 1.020 | 1.060 |
| | HS | 1.038 | 1.056 | 1.016 | 1.056 |
| | FER | 1.027 | 1.063 | 1.031 | 1.123 |
| 8×8 | ANS | 1.005 | 1.023 | 0.964 | 1.000 |
| | HS | 1.005 | 1.022 | 0.963 | 0.999 |
| | FER | 1.006 | 1.045 | 0.974 | 1.064 |
| 12×12 | ANS | 0.999 | 1.016 | 0.954 | 0.990 |
| | HS | 0.999 | 1.016 | 0.953 | 0.989 |
| | FER | 1.002 | 1.042 | 0.964 | 1.056 |

*Electric potential distribution*. Figures 6 to 9 illustrate the through-thickness electric potential fundamental mode for the laminated [1/2/2/1] and [2/1/1/2] plates for two aspect ratios under open-circuit condition, respectively. The linear electric potential distributions are also included in the figures to compare purpose. Plots of through-thickness electric potential fundamental mode for laminated [p/0/90/0/p] for both electric boundary conditions are shown in Figure 10 for *a*/*h*=4 and in Figure 11 for *a*/*h*=50. The curves in these figures have very similar shape with the exact solutions [11] and the FE results [3]. As seen in Figures 10 and 11 the electric conditions have a definite effect on electric fields in the piezoelectric layers. It is interesting to note that electric fields exist in the piezoelectric layers even with the closed-circuit conditions. Although the electric potential in piezoelectric layer is much lower in closed-circuit condition than in open-circuit-condition, it should not be neglected when the piezoelectric layer is thicker. It is noteworthy that the electric fields in piezoelectric layers have considerable difference between linear distribution and nonlinear distribution, especially, for electric field in middle piezoelectric layer (shown as Figures 6 to 9). 11 are calculated by using of hybrid stress method HS and 8×8 uniform meshes in-plane.

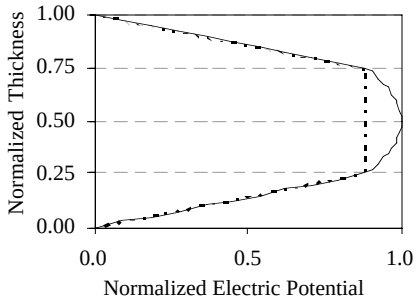


Figure 6. Through-thickness electric potential distributions for three-ply [1/2/2/1], a/h=4
(— nonlinear distribution, ------ linear distribution)

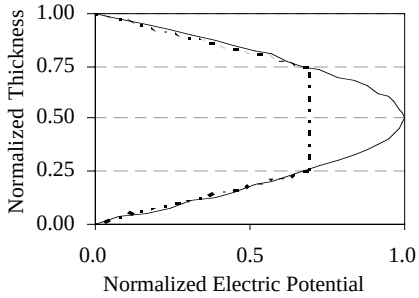


Figure 7. Through-thickness electric potential distributions for three-ply [1/2/2/1], a/h=50
(— nonlinear distribution, ------ linear distribution)

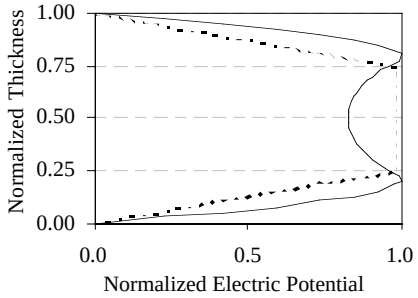


Figure 8. Through-thickness electric potential distributions for three-ply [2/1/1/2], a/h=4
(— nonlinear distribution, ------ linear distribution)

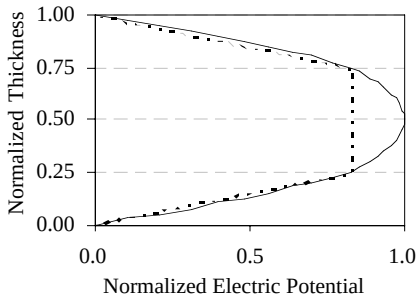


Figure 9. Through-thickness electric potential distributions for three-ply [2/1/1/2], a/h=50

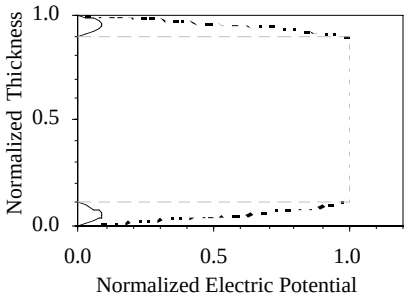


Figure 10. Through-thickness electric potential distributions for five-ply [p/0/90/0/p] for a/h=4
(— closed-circuit; ------ open-circuit)

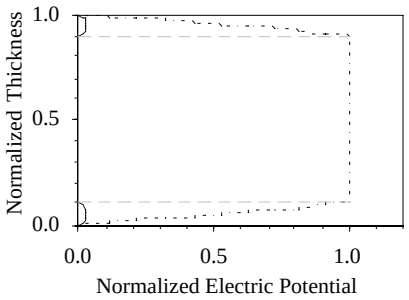


Figure 11. Through-thickness electric potential distributions for five-ply [p/0/90/0/p] for a/h=50
(— closed-circuit; ------ open-circuit)

## 9. CLOSURE

In this paper, an eight-node hexahedral solid-shell element for laminated composite structures is employed. The generalized laminate stiffness matrices are derived by the assumed natural strain method and hybrid stress method. The developed finite element models can resolve thickness locking and some abnormalities of the solid-shell elements in laminated materials. The solid-shell elements are then generalized for modeling piezoelectric materials by including the electromechanical coupling. Unlike the conventional piezoelectric elements, the nonlinear electric potential distribution in piezoelectric layer is described by introducing internal electric potential. Moreover, the notion of electric nodes is introduced that can conveniently take into account the equipotential effect induced by the metallization coated on the piezoelectric material. The developed finite element models, especially, electric node model, have the advantages of simpler modeling and can obtain same effect that exact solution described. Several examples are examined to illustrate the accuracy and efficiency of the models for analysis of piezoelectric composite plates. The predicted results show that the effect on natural frequency and electric field caused by through-thickness nonlinear electric potential distribution is very small generally, especially, in case of thin plate and laminate composite structure with surface bonded piezoelectric patches. However this effect should be considered for electric potential distribution when the piezoelectric layer is thick and its electric properties are strong.

## REFERENCES

[1] K. Chandrashekhara and A.N. Agarwal, "Active vibration control of laminated composite plates using piezoelectric devices: a finite element approach," *Journal of Intelligent Material Systems & Structures.* **4**, 496-508 (1993).

[2] D.T. Detwiler, M.H. Shen and V.B. Venkayya, "Finite element analysis of laminated composite structures containing distributed piezoelectric actuators and sensors," *Finite Elements in Analysis and Design*. **20**, 87-100 (1995).

[3] D.A. Saravanos, P.R. Heyliger and D.A. Hopkins, "Layerwise mechanics and finite element for the dynamic analysis of piezoelectric composite plates," *Int. J. Solids Structures*. **34**, 359-378 (1997).

[4] W.S. Hwang and H.C. Park, "Finite element modelling of piezoelectric sensors and actuators," *AIAA*. **31**, 930-937 (1993).

[5] K.Y. Sze and L.Q. Yao, "Modeling smart structures with segmented piezoelectric sensors and actuators," *Journal of sound and Vibration*. **235**, 495-520 (2000).

[6] K.Y. Sze, L.Q. Yao and S. Yi, "A hybrid-stress ANS solid-shell element and its generalization for smart structure modeling – part II: smart structure modeling," *Inter.J. Numer. Methods Engrg*. **48**, 565-582 (2000).

[7] S. Yi, S.F. Ling and M. Ying, "Large deformation finite element analyses of composite structures integrated with piezoelectric sensors and actuators," *Finite Elements in Analysis and Design.* **35**, 1-15 (2000).

[8] S.K. Ha, C. Keilers and F.K. Chang, "Finite element analysis of composite structures containing distributed piezoelectric sensors and actuators," *AIAA*. **30**, 772-780 (1992).

[9] J. Kim, V.V. Varadan and V.K. Varadan, "Finite element modelling of structures including piezoelectric active devices," *International Journal of Numerical Methods in Engineering*. **40**, 817-832 (1997).

[10] H.S. Tzou and R. Ye, "Analysis of piezoelectric structures with laminated piezoelectric triangle shell elements," *AIAA*. **34**, 110-115 (1996).

[11] P.R. Heyliger and D.A. Saravanos, "Exact free-vibration analysis of laminated plates with embedded piezoelectric layers," *J. Acoustical Soc. Am*. **98**, 1547-1557 (1995).

[12] K.Y. Sze and A. Ghali, "An hexahedral element for plates, shells and beams by selective scaling," *International* Journal *of Numerical Methods in Engineering*. **36**, 1519-1540 (1993).

*in Engineering*. **40**, 1839-1856 (1997).
[14] K.Y. Sze and Y.S. Pan, "Hybrid finite element models for piezoelectric materials," *Journal Sound & Vibration*. **26**, 519-547 (1999).
[15] T.H.H. Pian, "Finite elements based on consistently assumed stresses and displacements," *Finite Elements in Analysis & Design*. **1**, 131-140 (1985).
[16] K.Y. Sze, "Efficient formulation of robust hybrid elements using orthogonal stress/strain interpolants and admissible matrix formulation," *Inter.J.Numer.Methods Engrg.* **35**, 1-20 (1992).